Self-assembled monolayer electrode of a diiron complex with a phenoxo-based dinucleating ligand: observation of molecular oxygen adsorption/desorption in aqueous media†‡

Tomohiko Inomata,*[a] Kazuma Shinozaki,[a] Yuya Hayashi,[a] Hidekazu Arii,[b] Yasuhiro Funahashi,[a] Tomohiro Ozawa[a] and Hideki Masuda*[a]

Received (in Cambridge, UK) 2nd August 2007, Accepted 31st October 2007
First published as an Advance Article on the web 9th November 2007
DOI: 10.1039/b711802c

The phenoxo-based dinucleating ligand, 2,6-bis[bis(6-pivalamido-2-pyridylmethyl)amino-methyl]-4-aminophenol (1), and its Fe_2(II) complex, $[Fe_2(II)(1)(PhCOO)_2](CF_3SO_3)$ (2), were prepared and 2 deposited on the Au surface (2/Au) is much more stable than in solution and exhibits redox behavior in aqueous media as well as reversible adsorption/desorption of oxygen at room temperature.

The capture, release and activation of molecular oxygen are critical processes which must be considered for the development of applications such as oxygen sensors and fuel cell cathodes.[1,2] Various metal-containing proteins contribute to these processes in biological systems. In particular, iron-containing proteins play important roles in the storage, transport and activation of O_2.[3] Since investigations of functional model complexes aid in the elucidation of the mechanisms of biological systems, numerous studies of functional model complexes as models for the active centers of heme and non-heme enzymes have been reported.[4,5] Examples of immobilization of these model complexes onto substrates such as electrode surfaces have also been studied.[6] In these studies, the complexes are stabilized and in some cases display unique reactivity that is not observed in homogeneous solution.

We have previously reported Fe_2(II) non-heme enzyme model complexes with a dinucleating ligand that includes bulky pivalamide groups on its pyridine rings.[7] These Fe_2 complexes react irreversibly with O_2 to form stable μ-1,2-peroxo complexes at low temperatures. It is expected that the complexes deposited on the electrode will gain increased stability and react with O_2 at room temperature in aqueous media, while this electrode can provide electrons to these complexes and activate the bound dioxygen. Our goal is to use these non-heme functional model complexes in aqueous media for the development of devices capable of capturing and activating O_2.

We report herein the construction of a self-assembled monolayer (SAM) of diiron complexes with a phenoxo-based dinucleating ligand. The newly synthesized dinucleating ligand was deposited onto the electrode surface. Investigations indicate that the Fe_2 core displays redox behavior in aqueous media at room temperature with reversible adsorption/desorption of O_2.

The ligand **1** which includes a terminal amino group was prepared using a modification of previous methods (see ESI†).[7] After stirring a CH_2Cl_2–MeOH solution containing **1** (0.10 mmol), sodium benzoate bridging reagent (0.20 mmol), $Fe(CF_3SO_3)_2$ (0.20 mmol) and Et_3N (0.10 mmol) for a few hours in a glove box, the target Fe_2 complex **2** was obtained as yellow prismatic crystals. The product was characterized by IR and ESI-TOF MS spectroscopy and elemental analysis.§ The X-ray structure of **2** is indicated in Fig. S1† and exhibits two Fe centers bridged by two benzoate groups and one phenoxo group.¶ The formal charge of each Fe center is 2+ due to the presence of a $CF_3SO_3^-$ counter anion. A hydrogen bond exists between the pivalamide group N–H site and the oxygen atom of the bridging benzoate.

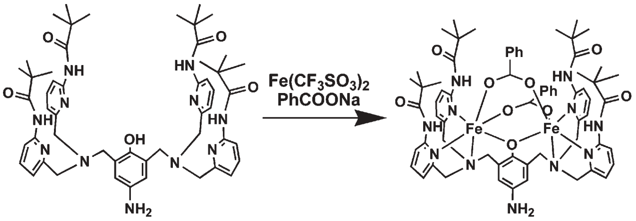

1 **2**

Fig. S2† shows the UV–vis spectrum of **2** in acetone under Ar and under saturated O_2 conditions. The spectrum of **2** drastically changed under saturated O_2 at −30 °C. The band observed around 600 nm is typical of phenoxo-bridged dinuclear Fe complexes reacting with molecular oxygen.[5] Two LMCT bands, which are assignable to 'peroxo to Fe(III) ion' and 'phenoxo to Fe(III) ion', overlapped in this region.[8] The resonance Raman spectrum of a similar Fe_2 complex, which has a CH_3-group instead of an NH_2-group at the *p*-position of phenolate, showed bands at 890 cm^{-1} for $^{16}O_2$ and at 840 cm^{-1} for $^{16}O_2$.[7] These values are typical of *cis*-μ-1,2-peroxo Fe_2 complexes.[5] However, this peroxo complex decomposes as the temperature increases to room temperature. A similar Fe_2(II) complex which does not contain pivalamide groups does not form a peroxo intermediate.[9] In these cases, Fe_2 complexes are only oxidized from the Fe_2(II,II) state to the Fe_2(II,III) state. This clearly indicates that the pivalamide groups contribute to the mechanism of the reaction with O_2. As was mentioned above, these pivalamide groups form hydrogen

---

[a] *Department of Applied Chemistry, Nagoya Institute of Technology, Gokiso-cho, Showa-ku, Nagoya, 466-8555, Japan.*
E-mail: masuda.hideki@nitech.ac.jp; Fax: +81-52-735-5209; Tel: +81-52-735-5228
[b] *Department of Chemistry, Gakushuin University, Mejiro, Toshima-ku, Tokyo, 171-8588, Japan*

† Electronic supplementary information (ESI) available: Preparation of **1**, X-ray crystal structure of **2**, UV–vis spectrum and CV of **2**, Table for the redox potential of **2**/Au. See DOI: 10.1039/b711802c

‡ The HTML version of this article has been enhanced with colour images.

bonds and allow the release of the bridging benzoate group. Consequently, **2** generates the peroxo complex under saturated O_2 conditions.

In cyclic voltammetry, one anodic wave and two cathodic peaks were observed at $E_{pa} = 0.43$ V and $E_{pc} = -0.16, 0.32$ V *vs.* Ag/Ag$^+$ (Fig. S3†). The anodic waves were compared twice to two other cathodic peaks. These waves are assignable to Fe$_2$(II,II/III,III), Fe$_2$(II,II/II,III) and Fe$_2$(II,III/III,III), respectively, which correspond well with those of previously reported Fe$_2$ complexes with similar structures.[7] These previously reported complexes had a terminal –CH_3 group instead of a terminal –NH_2 group at the *p*-position of phenolate. The redox behavior of Fe$_2$ complexes with pivalamide groups is complex and not as clearly defined as the redox behavior of the previously reported Fe$_2$ complexes. This complex electrochemical behavior of **2** is probably due to the pivalamide groups influencing the weakening of the Fe–O bond of bridging benzoate groups and causing loss of coordination of one of the bridging benzoate groups from the Fe center. Thus, several species coexist in each oxidation state of **2** and complicate the redox behavior. However, multiple cyclic voltammetry scans were essentially identical, indicating that decomposition of **2** in solution does not occur.

As described in the experimental section, **2** was deposited onto the Au electrode surface stepwise (Fig. 1). The Au electrode was dipped into dithiobis(succinimidyl carboxylate) (DTSC) solution (Fig. 1a). The resulting monolayer of TSC/Au (TSC, thiobis-(succinimidyl carboxylate) was immersed into the solution of **2** to produce the target Fe$_2$ complex-modified Au electrode, **2**/Au (Fig. 1b).‖ Two types of DTSC were used (DTSP and DTSU containing propionate and undecanoate linkers, respectively).

It is notable that the Fe$_2$ core of **2**/Au is remarkably stable in aqueous media. Fig. 2a shows a cyclic voltammogram of **2**/Au in 0.1 M aq. NaCF$_3$SO$_3$. The linear relationship between each scan rate and peak current indicates that these waves are derived from the species attached to the electrode surface.[10] The redox behavior is similar to that of **2** in homogeneous solution. However, all of the redox potentials of **2**/Au are markedly shifted in the negative direction. Although the cause of these negative shifts is not currently understood, Wackerbarth *et al.* reported a similar significantly negative shift of SAMs of Co$_2$ oxygen complexes which have a similar dinuclear ligand.[11] It was pointed out that the proximity of the peroxide ligand to the Au surface and the translocation of the surface charge to the peroxo group could provide an explanation for the negative shift. When the bridging benzoate in **2**/Au was substituted with *p*-MeO-benzoate or *p*-NC-benzoate, the redox potentials of each of the SAMs were altered in a manner that depends upon the substituent effect of the bridging benzoate group (Table S1†). Thus, we assign the redox waves I, II and III to Fe$_2$(II,II/III,III), Fe$_2$(II,III/III,III) and Fe$_2$(II,II/II,III), respectively.**

The surface coverage of the Fe$_2$ units on the Au electrode surface, which was estimated from the area of the redox wave, was calculated to be *ca.* $3–4 \times 10^{-11}$ mol cm^{-2}. Considering the ideal coverage calculated from the projection area of **2** (4.0×10^{-11} mol cm^{-2}, estimated from the X-ray crystallography of **2**), the complex is quite densely packed on the electrode surface. **2** is difficult to dissolve in H_2O and is easily oxidized which causes decomposition in solution in the presence of even trace amounts of oxygen and/or moisture. The high stability of the **2**/Au complex is most likely caused by the dense packing and hydrophobic interactions of the Fe$_2$ complex in **2**/Au. These effects partially protect the Fe$_2$ complex from attack by H_2O and O_2. Consequently, the Fe$_2$ units in **2**/Au are very stable with regard to reactivity with O_2. The difference in the lengths of DTSC also contributes to the stability of **2**. A multi-cycled CV measurement indicated that **2**/Au formed with DTSU, which has a nine-carbon chain, is more stable than that formed with DTSP, which has only an ethylene chain. This stability most likely originates from the contribution of van der Waals interactions among the alkyl chains of DTSC.

Under saturated O_2 conditions, the CV of **2**/Au is drastically altered in aqueous solution, indicating the occurrence of binding of O_2 (Fig. 2b). The areas of waves IV and V under saturated O_2 were almost the same as those of I, II under Ar. Thus, the waves IV

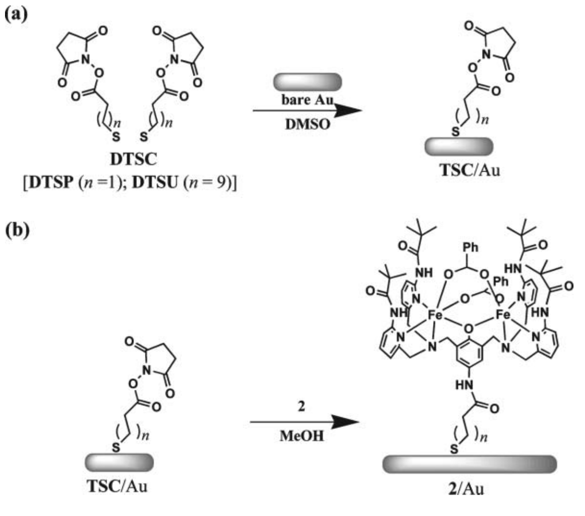

Fig. 1 Schematic views of the process of surface modification with **2**. (a) Self-assembly of the TSC monolayer on the bare Au electrode by spontaneous splitting of the DTSC. (b) Cross-linking of **2** with the TSC monolayer.

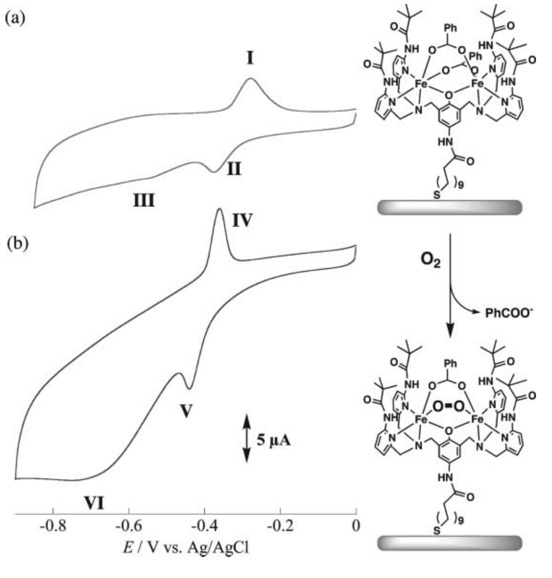

Fig. 2 Cyclic voltammograms of **2**/Au (constructed with DTSU) in aqueous media (pH 6.0) under (a) Ar and (b) saturated O_2 conditions, respectively. Scan rate is 50 mV s^{-1}.

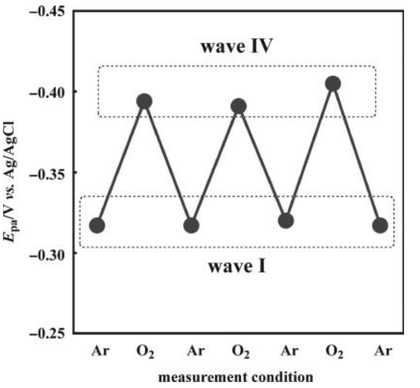

Fig. 3 Plot of the redox potential of Fe_2(II,II/III,III) on **2**/Au (constructed with DTSP). The wave designated 'IV' was obtained after a flash of O_2 gas for 20 s. The wave designated 'I' was obtained after bubbling with Ar for 10 min.

($2e^-$) and V ($1e^-$) were assigned to the waves of μ-1,2-peroxo complexes, $Fe_2(O_2)$(II,II/III,III) and $Fe_2(O_2)$(II,III/III,III), respectively. It is very important that this voltammogram showed reversible changes. Fig. 3 shows the plot of the redox potentials of I and IV, which indicate the redox wave of Fe_2(II,II/III,III) under Ar and saturated O_2 conditions. From this plot it can be seen that the redox waves observed under Ar shift to the negative region under saturated O_2 conditions. The redox wave shift under saturated O_2 occurs after bubbling of Ar. This finding indicates that reversible O_2 adsorption/desorption occurs on **2**/Au in aqueous media at room temperature.

It is interesting to note that the wave designated VI is very large compared to other waves. The relative current of VI increases with slower scan rates. Moreover, this current also increases with decreasing pH of the electrolyte. This indicates that the catalytic wave represents reduction of O_2 to H_2O_2 and/or H_2O. Preliminary experiments using rotated ring-disk electrodes indicated that O_2 binding to **2**/Au on the disk electrode is detected as H_2O_2 or O_2^{2-} at the ring electrode. Thus, **2** has the potential to bind molecular O_2 and to reduce it electrocatalytically. Unfortunately the redox potential of the wave VI was quite negative. In this potential region, a bare Au electrode can also reduce molecular O_2 to H_2O_2. Because the starting potential of the catalytic wave of **2**/Au depends upon the redox potential of **2**, the observed catalytic wave originates from the **2**/Au electrode. This result indicates that **2**/Au can activate molecular oxygen to at least O_2^{2-}. Since the redox potential of this catalytic wave is quite negative, **2**/Au is not currently applicable as an O_2 activation method. We are continuing to develop useful Fe_2 complexes that activate O_2 at more positive potentials.

In summary, we developed a Au electrode modified by deposition of a non-heme functional model Fe_2 complex with a phenoxo-based dinucleating ligand and observed a rare example of reversible oxygen adsorption/desorption in aqueous media at room temperature. Immobilization of the complex onto the electrode surface was found to greatly stabilize **2**.

This work was supported partly by a Grant-in-Aid for Scientific Research from the Ministry of Education, Science, Sports, and Culture of Japan and partly by a grant from the NITECH 21st Century COE Program, to which our thanks are due.

Notes and references

§ Selective data for **2**: IR (KBr, cm^{-1}): 3436 (ν_{N-H}), 3341 (ν_{N-H}), 1692 ($\nu_{C=O}$), 1614 (ν_{COO}), 1415 (ν_{COO}), 1279 (ν_{C-F}), 1258 (ν_{C-F}), 1161 (δ_{S-O}), 1032 (ν_{S-O}), 639 ($\nu_{C=S}$). *m/z* (ESI-TOF MS) $[M - CF_3SO_3^-]^+$: 1280.6. Found: C, 55.97; H, 5.21; N, 10.57%. Calcd. for **2**·MeOH: C, 55.86; H, 5.65; N, 10.54%.

¶ CCDC 656303. For crystallographic data in CIF or other electronic format see DOI: 10.1039/b711802c

‖ Preparation of deposited **2**/Au: Au film with a thickness of 1000 Å was deposited onto a cleaved mica substrate (14 × 14 mm) at 1.0 Å s^{-1} by a JIS-300AK vacuum coater (Sinku Technology Co., Ltd.). The Au film was annealed with a hydrogen gas flame before it was dipped into each sample solution. TSC/Au was prepared by immersing the Au film into a 2 mM solution of DTSC in DMSO for 5 min. After washing with DMSO and H_2O, the resulting TSC/Au preparation was dipped into 1 mM **2** in H_2O and left to stand for 1 day.

** Electrochemical measurements were performed by using an ALS-600 electrochemical analyzer (BAS Inc.). The cyclic voltammograms were recorded using a glassy carbon electrode or each SAM as a working electrode, Pt wire as a counter electrode and Ag/Ag^+ (0.01 M $AgNO_3$ in acetonitrile) or Ag/AgCl (3 M NaCl) as a reference electrode. A 0.1 M solution of $TBA(CF_3SO_3)$ in CH_2Cl_2 or a 0.1 M $NaClO_4$ aqueous solution was used as an electrolyte. Rotating ring-disk electrode measurements were performed using a Hokutodenko HR-201 electrode motor and a Hokutodenko HR-202 rotation controller with a Hokutodenko HZ-5000 electrochemical analyzer. A ring-disk electrode (Au disk (ø 5.0 mm) and Pt ring (ø 6.8 mm with 1.2 mm width), available from Hokutodenko) was modified by deposition of **2** in the manner described above. All measurements were performed under a rigorous Ar atmosphere.

1 I. Fatt, *Polarographic Oxygen Sensors*, CRC Press, Cleveland, 1976; *Polarographic Oxygen Sensors: Aquatic and Physiological Applications*, ed. E. Gnaiger and H. Forstner, Springer-Verlag, Berlin, 1983.
2 B. C. H. Steel and A. Heinzel, *Nature*, 2001, **414**, 345–352; N. P. Brandon, S. Skinner and B. C. H. Steele, *Annu. Rev. Mater. Res.*, 2003, **33**, 183–213.
3 *Bioinorganic Chemistry*, ed. I. Bertini, H. B. Gray, S. J. Lippard and J. Valentine, University Science Books, Mill Valley, 1994.
4 M.-A. Kopf and K. D. Karlin, *Inorg. Chem.*, 1999, **38**, 4922–4923; Y. M. Goh and W. Nam, *Inorg. Chem.*, 1999, **38**, 914–920; J. P. Collman, R. Boulatov, C. J. Sunderland and L. Fu, *Chem. Rev.*, 2004, **104**, 561–588.
5 N. Kitajima, N. Tamura, H. Amagi, H. Fukui, Y. Moro-oka, Y. Mizutani, T. Kitagawa, R. Mathur, K. Heerwegh, C. A. Reed, C. R. Randall, L. Que, Jr. and K. Tatsumi, *J. Am. Chem. Soc.*, 1994, **116**, 9071–9085; K. Kim and S. J. Lippard, *J. Am. Chem. Soc.*, 1996, **118**, 4914–4915; T. Ookubo, H. Sugimoto, T. Nagayama, H. Masuda, T. Sato, K. Tanaka, Y. Maeda, H. Okawa, Y. Hayashi, A. Uehara and M. Suzuki, *J. Am. Chem. Soc.*, 1996, **118**, 701–702; Y. Dong, S. Yan, V. G. Young, Jr. and L. Que, Jr., *Angew. Chem., Int. Ed. Engl.*, 1996, **35**, 618–620.
6 T. Inomata, M. Abe, T. Kondo, K. Umakoshi, K. Uosaki and Y. Sasaki, *Chem. Lett.*, 1999, 1097–1098; R. Boulatov, J. P. Collman, I. M. Shiryaeva and C. J. Sunderland, *J. Am. Chem. Soc.*, 2002, **124**, 11923–11935; A. K. Udit, W. Belliston-Bittner, E. C. Glazer, Y. H. L. Nguyen, J. M. Gillan, M. G. Hill, M. A. Marletta, D. B. Goodin and H. B. Gray, *J. Am. Chem. Soc.*, 2005, **127**, 11212–11213; C. M. Codas, A. S. Viana, S. Leupold, F.-P. Montforts and L. M. Abrantes, *Electrochem. Commun.*, 2006, **5**, 36–41.
7 H. Arii, S. Nagatomo, T. Kitagawa, T. Miwa, K. Jitsukawa, H. Einaga and H. Masuda, *J. Inorg. Biochem.*, 2000, **82**, 153–162; S. Ishikawa, *Master's thesis*, Nagoya Institute of Technology, 2003.
8 Y. Dong, S. Menage, B. A. Brennan, T. E. Elgren, H. G. Jang, L. L. Pearce and L. Que, Jr., *J. Am. Chem. Soc.*, 1993, **115**, 1851–1859; E. Lambert, B. Chabut, S. Chardon-Noblat, A. Deronzier, G. Chottard, A. Bousseksou, J.-P. Tuchagues, J. Laugier, M. Bardet and J.-M. Latour, *J. Am. Chem. Soc.*, 1997, **119**, 9424–9437.
9 H. Sugimoto, T. Nagayama, S. Maruyama, S. Fujinami, Y. Yasuda, M. Suzuki and A. Uehara, *Bull. Chem. Soc. Jpn.*, 1998, **71**, 2267–2279.
10 A. J. Bard and L. R. Faulkner, *Electrochemical Methods: Fundamentals and Applications*, Willy, New York, 2nd edn, 2001.
11 H. Wackerbarth, F. B. Larsen, A. G. Hansen, C. J. McKenzie and J. Ulstrup, *Dalton Trans.*, 2006, 3438–3444.